

RESEARCH

Open Access



The potentials of nonlinear polarization with hyperspectral imaging of RNA for hepatocellular carcinoma early diagnosis

Yasser H. El-Sharkawy¹, Sherif Elbasuney², Sara M. Radwan³, Mostafa A. Askar⁴, Samar H. Rizk^{5,6} and Gharieb S. El-Sayyad^{7,8,9*}

Abstract

Background Most cancers acquire numerous genetic changes in proto-oncogenes as well as tumor-suppressor genes. Cancer's early diagnosis remains a challenge. Recently, nonlinear polarization has revealed the potential as a promising tool for early cancer diagnosis. Laser-induced nonlinear polarization can offer a novel fingerprint signature.

Methods In this study, nonlinear polarization was adopted for the characterization of both DNA and RNA samples from healthy volunteers. Total DNA and RNA were illuminated with a 656-nm LED source, and the resonance frequencies (scattered and re-emitted signals) were captured and recorded using a hyperspectral camera.

Results Changes in signal frequency as well as phase shift offered a potent means to differentiate DNA (control) from RNA (control). DNA (control) demonstrated characteristic resonance frequencies that differ from total RNA (control) at the 2nd, 3rd, 4th, and 5th harmonics. While DNA demonstrated a phase shift dominating at 0.88 GHz, RNA dominates at 0.106 GHz. The resonance spectral signature of RNA samples from people with hepatocellular carcinoma (HCC) was compared to that of RNA (control). RNA (HCC) demonstrated distinctive frequency signals at 0.014, 0.021, 0.032, and 0.072 GHz. These characteristics feature could facilitate early HCC diagnosis. While RNA (control) dominates at 0.014 and 0.072 MHz, RNA (HCC) dominates at 0.021 and 0.032.

Conclusion As far as we are aware, this is the initial investigation into the use of simple nonlinear polarization to generate spectral fingerprinting signatures of total DNA and RNA. Furthermore, RNA mutations due to HCC were identified via characteristic nonlinear spectral signature.

Keywords Spectroscopy, Total RNA, Genetic changes, Cellular carcinoma, Hyperspectral imaging

*Correspondence:

Gharieb S. El-Sayyad
adham_adham699@yahoo.com

¹ Optoelectronics Department, Military Technical College, Cairo, Egypt

² Head of Nanotechnology Research Center, Military Technical College, Cairo, Egypt

³ Biochemistry Department, Faculty of Pharmacy, Ain Shams University, Cairo, Egypt

⁴ Radiation Biology Department, National Center for Radiation Research and Technology (NCRRT), Egyptian Atomic Energy Authority (EAEA), Cairo, Egypt

⁵ Department of Biochemistry, Faculty of Pharmacy, Ahrum Canadian University, Sixth October City, Giza, Egypt

⁶ Department of Biochemistry, Faculty of Pharmacy, Galala University, New Galala City, Suez, Egypt

⁷ Department of Microbiology and Immunology, Faculty of Pharmacy, Galala University, New Galala City, Suez, Egypt

⁸ Department of Microbiology and Immunology, Faculty of Pharmacy, Ahrum Canadian University, Sixth October City, Giza, Egypt

⁹ Drug Radiation Research Department, National Center for Radiation Research and Technology (NCRRT), Egyptian Atomic Energy Authority (EAEA), Cairo, Egypt

Introduction

Cancer is driven by genetic mutations which affect cell proliferation and survival [1]. Genes that play a significant part in the development of cancer, fall into two basic categories: tumor-suppressor genes and proto-oncogenes [2]. Both classes encode several proteins which control cell growth, proliferation, DNA repair, invasion, motility, angiogenesis, apoptosis, and several other cellular processes; mutations of which can contribute to cancer development. These mutations work collectively for cancer progress [3]. Additionally, somatic variations in cancer genomes cause RNA alterations, including over-expression, splicing mutations, or gene fusions [4]. The significance genetic alterations on the growth of malignancies have become the subject of several studies. Hepatocellular carcinoma (HCC) is one of the most common, deadly, and rapidly spreading malignancies [5, 6]. HCC early diagnosis is significant to improve the prognosis and patient survival. HCC diagnosis depends mainly on imaging techniques including ultrasonography, magnetic resonance imaging, and computed tomography. However, early HCC diagnosis remains a challenge [7].

Nonlinear polarization is a benign, noncontact, and nonionizing modality [8, 9]. This modality has found wide applications particularly in disease diagnosis and image-guided surgeries [8], as different materials can expose different responses (reflection, absorption, and scattering) to stimulating light [10]. Nonlinear polarization can secure diagnostic characteristic signatures to differentiate between normal and tumor tissues [11]. The incident electric field $|E|$ can induce distinctive zones of positive and negative charges [8–10]. The intensity of the applied electric field $|E|$ determines how much charge polarization could be developed in any particular material [11, 12]. The generated dipole moment can switch its energy and release an electric field at the exact same frequency (Rayleigh scattering) [13–16]. Strong stimulating light and macromolecule could interact more effectively in nonlinear polarization, with the evolution of characteristic signatures [17]. Numerous molecules can be stimulated by strong irradiation; the excited state can then serve as the low energy state for an extra stimulation [18]. The intense light interaction can result in the generation of new resonance frequencies related to all energy differences. Nonlinear polarization includes strong stimulating electric field, with the evolution of new electric waves. The candidate materials for second-order nonlinear polarization are molecules with significant charge transfer and electronic transitions [19]. On the other hand, hyperspectral imaging (HSI) is a powerful noninvasive optical technique for numerous biomedical applications [20–23]. HSI can be employed for tumor diagnosis and detection during surgical operations [24–26]. HSI is

candidate for morphological and biochemical information of biological tissues; it can enable a coincident collective measurement of both spatial and spectral data [20, 21]. HSI can offer precise measurement of characteristic RNA optical signatures. Moreover, mutations in RNA structure due to HCC could be precisely monitored via nonlinear polarization signatures. The change of incident electric field amplitude causes the induced dipoles to oscillate [24–26]. Intense electric field can secure nonlinear polarization with the generation of new frequencies [19]. RNA mutations due to HCC could alter the nonlinear polarization response. Such response could provide virtual fingerprint information for normal and cancerous macromolecules [17]. In this study, optical approach based on nonlinear polarization is described as a prominent platform for the spectroscopic and spatial characterization of DNA and RNA in HCC patients.

Subjects and methods

Subjects

This study included five male patients with primary HCC, whose diagnosis was established in accordance with the EASL's recommendations and on the basis of histological sample. Five healthy male volunteers of similar ages were also recruited in the research as healthy controls. Every individual gave his informed agreement, and the study was authorized by the Ain-Shams University Hospitals' ethical committee for research. Furthermore, the study was conducted in accordance with the guidelines and suggestions of the Declaration of Helsinki.

Laboratory examines

Two blood samples were taken from each participant to prepare whole blood in vacutainer tubes with sodium salt of ethylene-diamine-tetra-acetic acid ($\text{Na}_2\text{-EDTA}$, final concentration of 1.5 mg/mL), an agent that prevents blood clots by binding to calcium in the blood. Total RNA was purified from whole blood and the entire blood count was measured.

Complete blood count (CBC) investigation

The Z2TM Coulter Counter[®], Analyzer, Coulter Electronics, USA, was used to measure total leukocyte count (TLC), hemoglobin (Hgb), red blood cell (RBC) count, and platelet count (PLT).

Genomic DNA extraction and total RNA purification

Following the manufacturer's instructions, genomic DNA was isolated using the QIAamp DNA Mini-Kit technique (Qiagen, Hilden, Germany). DNA samples were quantified and their purity was evaluated using the NanoDrop[®] (ND)-1000 spectrophotometer (Nano-Drop Technologies, Inc., Wilmington, DE, USA). Using a QIAamp RNA

blood mini-kit (Qiagen, Hilden, Germany), total RNA was extracted and purified in accordance with the manufacturer’s instructions.

Nonlinear polarization measurements

Biomedical applications for nonlinear polarization are appealing. This method can provide extensive knowledge on the chemical and physical characteristics of whole DNA and RNA. A tiny lens was utilized to concentrate a laser source (10 mw at 656 nm) in order to excite the evaluated total DNA and RNA samples. A hyperspectral camera was used to gather the resonance frequency (scattered and re-emitted). Hyperspectral camera, with 3.16 nm resolution, was employed to acquire resonance frequencies over the range 395: 1100 nm (Fig. 1).

The collected signals were analyzed via customized digital signal processing technique for frequency domain evaluation. This algorithm was employed to evaluate the phase difference between total DNA, RNA (control). Mutation in RNA macromolecule structure due to gene disorder could result in change in optical properties with change nonlinear polarization signature and phase shift. Signature change of RNA due to HCC mutation was captured and processed. The phase and frequency responses were calculated in an attempt to determine both DNA and RNA spectral signature. This characteristic may serve as a baseline to track any genetic modifications to total RNA structure due to HCC tumors.

Statistical analysis

The SPSS statistics program version-23 software package (SPSS Inc., Chicago, IL, USA) was used for all statistical analyses. The data are shown as mean SD. Using the (HCC) group as the comparison group, statistical significance between all groups was examined (**p* 0.001, ***p* 0.01, #*p* 0.05). The Pad-Prism software programmer, version 8 (Graph-Pad Software, La Jolla, CA), was used to create statistical analysis graphics.

Results and discussion

Participants’ clinical and demographic features

The field of care testing toward the analysis of blood lack nowadays raped and simple test techniques for biomarkers. In this study, we have developed a novel DNA/RNA genetic signature via nonlinear polarization with hyperspectral imaging for helping hepatocellular carcinoma early diagnosis.

Table 1 Clinical and demographic data characteristics

Features	Control group	HCC group
Age (years)	51.9±2.3	52.3±1.9
Hemoglobin (g %)	14.3±1.9	13.1±1.8
RBCs (x 10 ⁶ cells/μL)	4.3±0.7	4.1±0.9
TLC (x 10 ³ cells/μL)	6.0±2.2	6.8±2.1
Platelet count (x 10 ³ cells/μL)	225±26.2	305±40.1

Data are presented as mean ± SD for five samples, *P* value ≤ 0.05

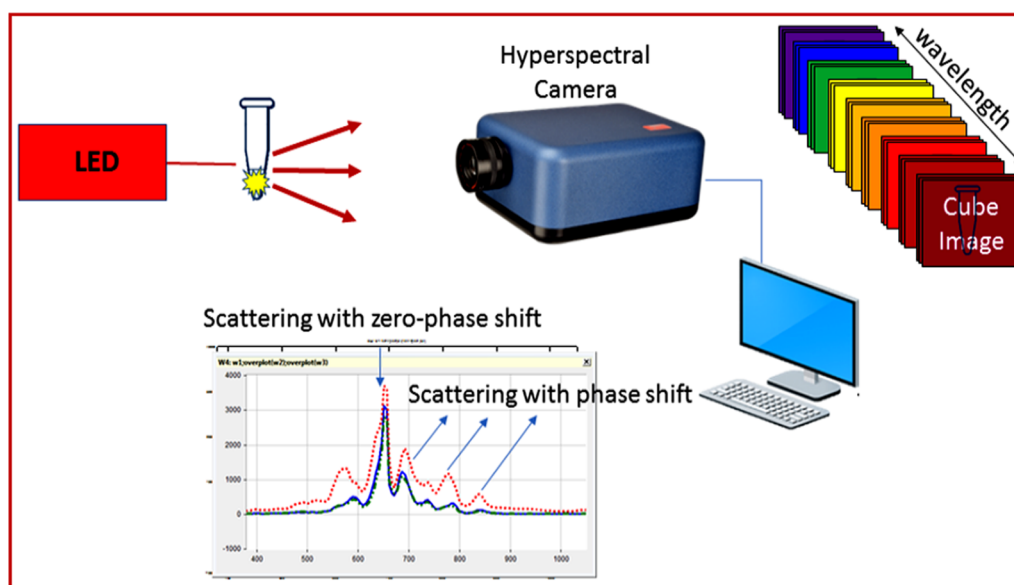


Fig. 1 Schematic illustration of nonlinear polarization measurements for total DNA and RNA

Table 1 presents the participant’s clinical and demographic details. According to a prior study, the higher baseline platelet level and lower baseline hemoglobin may be associated to possible prognostic factors for cancer.

Characterizing the nonpolarized signature of DNA/RNA control

The most prevalent malignant primary liver tumor is hepatocellular carcinoma (HCC) that usually develops from the progression of cirrhosis. In terms of the pathological observation, many pathological stain-based diagnosis studies are performed on tissue specimens and cells. Staining is time-consuming. With the help of hyperspectral imaging by light polarization signature of DNA/RNA in specimen, it is possible to observe specimens without staining or fixation.

A study by Hashimoto et al. [27] conducted a computer-aided diagnosis on liver pathological samples which were hematoxylin and eosin (H & E) stained. Applying hyperspectral imaging (HSI) to the same samples, the accuracy improvement has reached to 24% for fibers and 5% for cytoplasm. So, DNA/RNA genetic signature via nonlinear polarization with hyperspectral imaging is possible help to hepatocellular carcinoma early diagnosis.

Total DNA and RNA under polarized light can provide information regarding chemical structure links and dielectric characteristics. Light emission and absorption can be used to assess the dielectric characteristics of macromolecules. Due to mutations in macromolecule (DNA and RNA) chemical structure, the harmonic oscillation signature could offer a distinctive signature [28]. The scattered and re-emitted fingerprint for total DNA and RNA (control) is demonstrated in Fig. 2 (mean of 5 samples).

In an attempt to conclude spectral oscillation signature, normalized (scattered and re-emitted) signatures were calculated to investigate polarized light intensity (Fig. 3).

Light polarization signature of DNA/RNA (control)

Nonpolarized signature of total DNA and RNA could be employed to offer platform for determining the spectral fingerprint signature of both total DNA and RNA. Characteristic resonance frequency for each sample is represented in Table 2.

Total DNA demonstrated characteristic resonance frequencies that differ from total RNA at 2nd, 3rd, 4th, 5th harmonic. Variable polarization states can be noticed by varying the total DNA and RNA structural arrangement with variable light absorption (attenuation). Signal

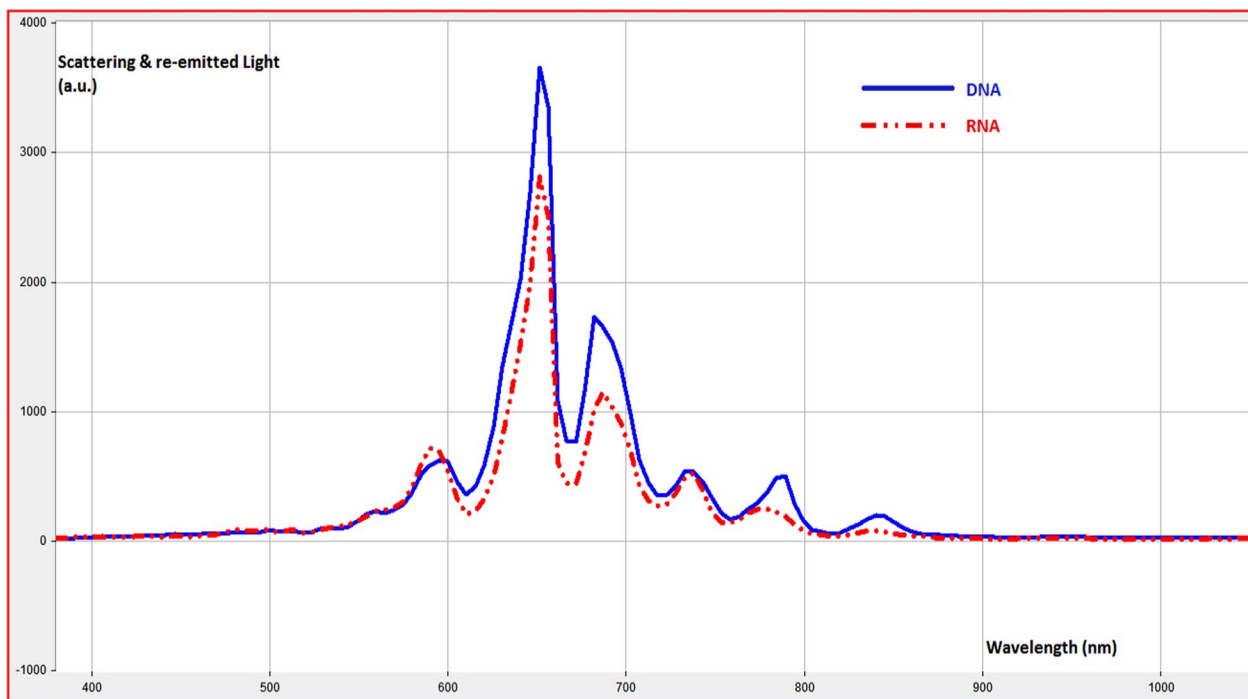


Fig. 2 Resonance harmonic oscillations of whole DNA and RNA (control) samples irradiated by a laser source at 656 nm (scattered and returned energy)

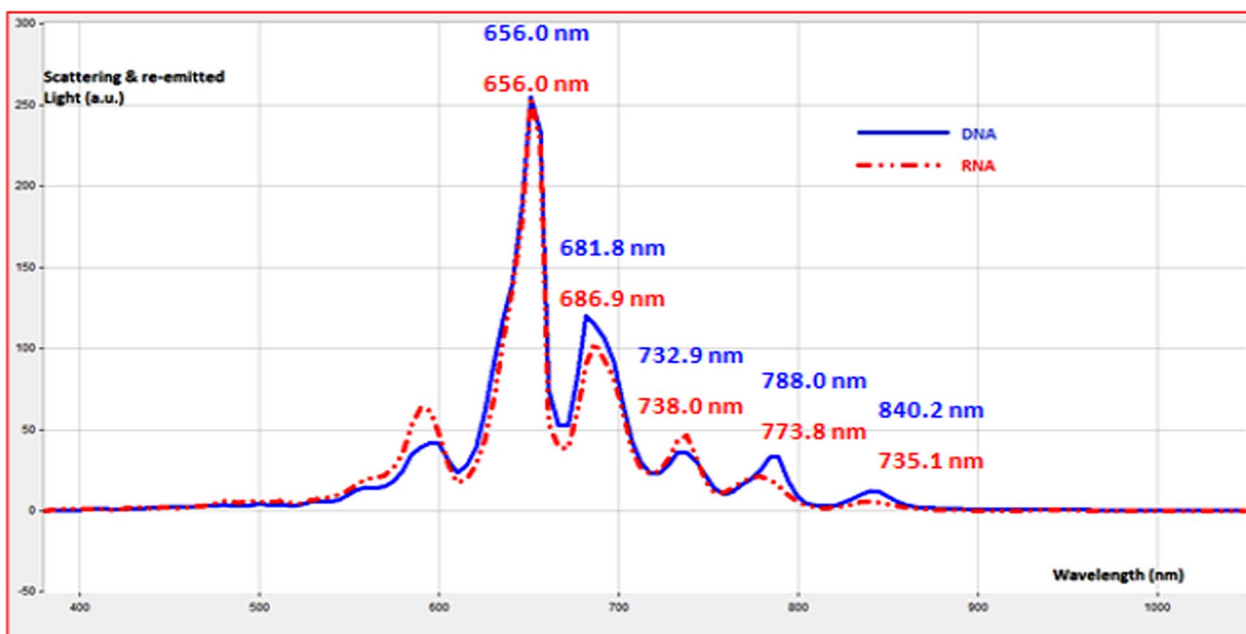


Fig. 3 Normalized harmonic oscillations (scattered and re-emitted radiation) of total DNA and RNA (control) after being irradiated with laser source at 656 nm

Table 2 Characteristic light polarization signature of total DNA/RNA (control)

Sample	Rayleigh scattering (nm)	Re-emitted radiation (2nd harmonic) (nm)	Re-emitted radiation (3rd harmonic) (nm)	Re-emitted radiation (4th harmonic) (nm)	Re-emitted radiation (5th harmonic) (nm)
DNA	656.0	681.8	732.9	788.0	840.2
RNA	656.0	686.9	738.0	773.8	835.1

Table 3 Attenuation of transmitted light polarization of total DNA and RNA samples

Sample	Rayleigh scattering (intensity a.u.)	Re-emitted radiation (2nd harmonic) (intensity)	Re-emitted radiation (3rd harmonic) (intensity)	Re-emitted radiation (4th harmonic) (intensity)	Re-emitted radiation (5th harmonic) (intensity)
DNA	3653	1738	545	503	201
RNA	2794	1163	545	301	76

intensity of total DNA and RNA signature is demonstrated in Table 3. Nonpolarized signature attenuation offered another path to differentiate between total DNA and RNA spectral signatures.

Frequency changes and phase differences of DNA/RNA (control)

In an effort to distinguish between the spectral fingerprint characteristics of total DNA and RNA control samples via change in frequency response, harmonic oscillations (scattered and re-emitted) radiations were processed using rapid Fourier transform (Fig. 4).

Briefly, for the first time, blood analysis by nonlinear polarization with hyperspectral imaging has demonstrated the potential use of DNA/RNA genetic signature in blood spectral biomarkers as a novel alternative for hepatocellular carcinoma diagnosis, which could be used for screening purposes.

Total DNA demonstrated characteristic frequency response that could be discriminated from total RNA. DNA demonstrated spectrum band starting from 0.0044 to 0.0118 GHz compared with RNA spectrum lines. In an attempt to explicitly discriminate between total DNA and RNA, phase change was investigated. Change in frequency signal phase can be considered as a potent tool to discriminate the spectral signatures of both total DNA and RNA (Fig. 5). DNA can be efficiently distinguished from RNA via phase shift. While DNA demonstrated phase shift dominates at 0.088 GHz, RNA dominates at 0.106 GHz (Fig. 5). These stage shifts could be attributed to DNA's distinct chemical composition and dielectric features from RNA.

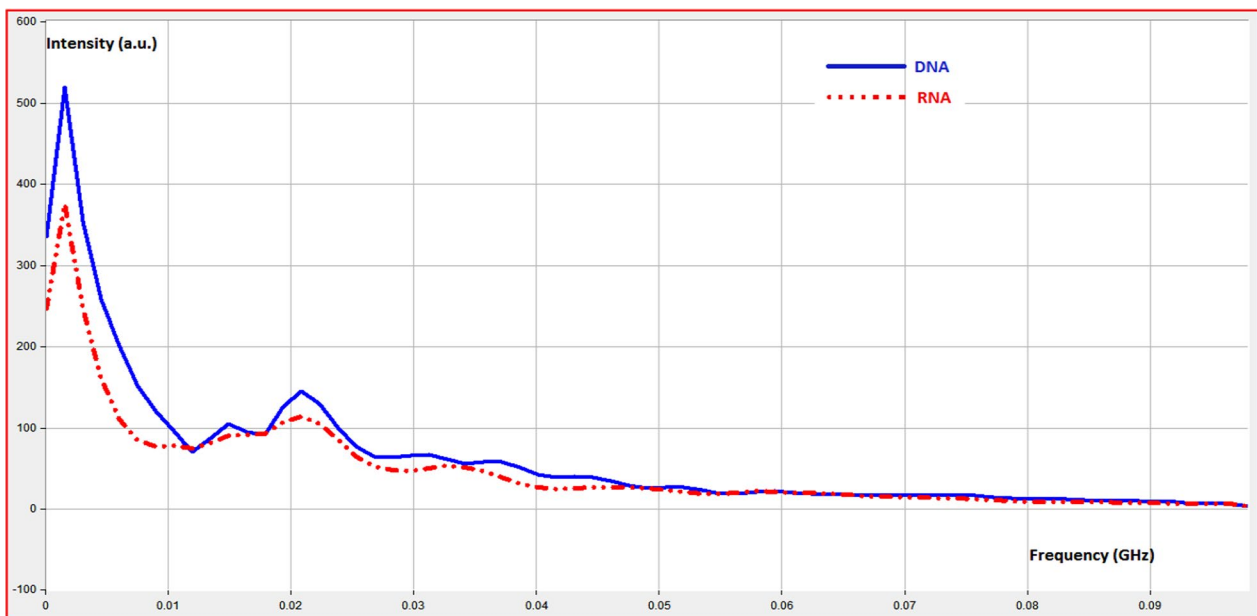


Fig. 4 Frequency change of total DNA and RNA (control)

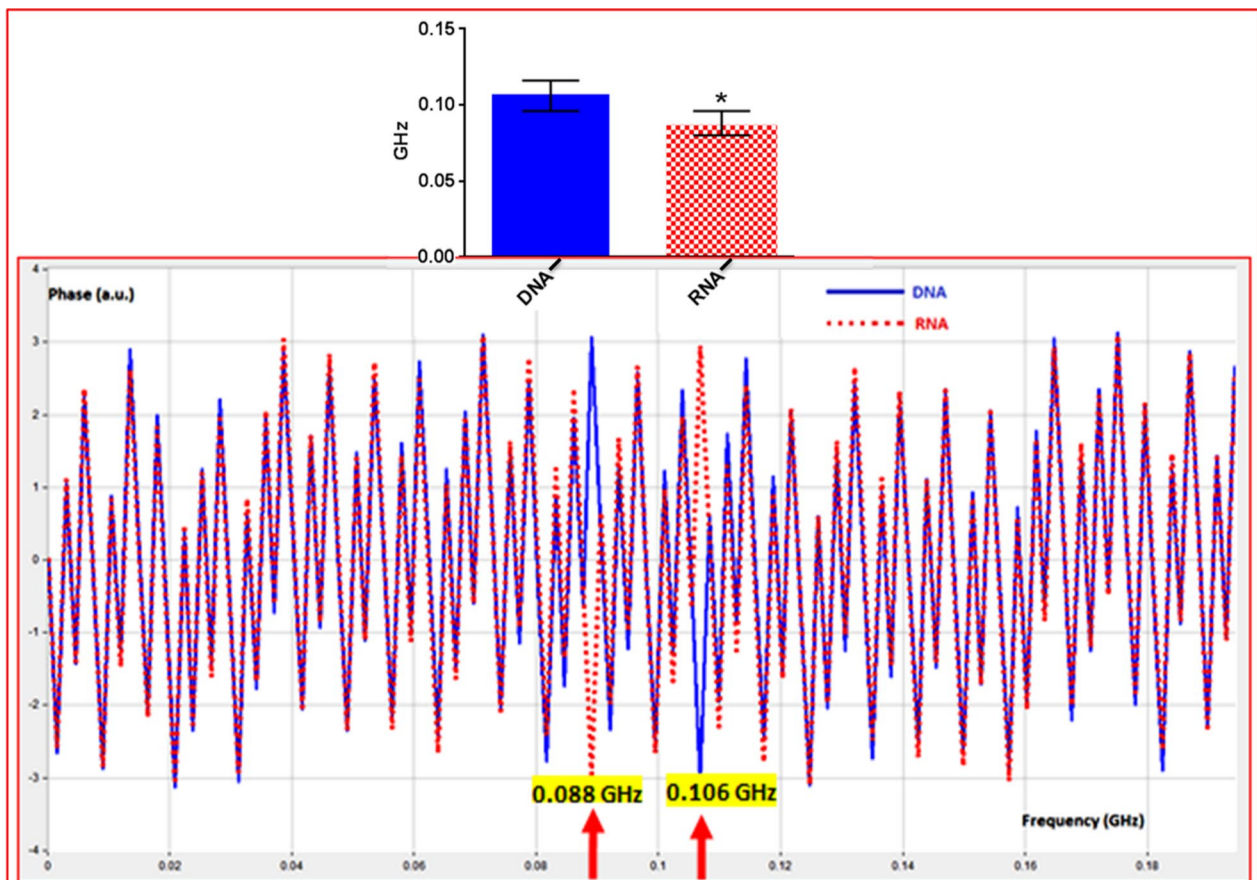


Fig. 5 Phase difference between DNA and RNA

Impact of HCC tumor on RNA nonlinear polarization signature

The optoelectronic and dielectric characteristics of RNA may change along with HCC-related changes. Re-emitted light radiation at resonance frequencies could provide a fingerprint sign for chemical composition and physical characteristics. The nonlinear response of RNA (control) was investigated to RNA (HCC) for early HCC diagnosis (Fig. 6).

To counteract the impact of the intensity of polarized light, normalized signatures (scattered and re-emitted radiations) were determined (Fig. 7).

The re-emitted signature could be distinguished due to changes in molecular-electronic configuration and absorber size in the order of (nm). The resonance frequency for RNA (control) to RNA (HCC) is shown in Table 4.

Various polarization states produced by various structural configurations can exhibit variable light attenuation. Table 5 lists the attenuation of the investigated samples.

Impact of HCC tumor on RNA frequency changes and phase differences

To distinguish between RNA (control) and RNA (HCC), nonlinear signature was processed using a quick Fourier transform. RNA (HCC) demonstrated characteristic frequency signals at 0.006, 0.014, and 0.022 MHz. These signals could offer good discrimination between RNA (HCC) and RNA (control) (Fig. 8).

Phase difference between RNA (control) and RNA (HCC) was investigated. Whereas RNA (control) dominates at 0.014 and 0.072 MHz, RNA (HCC) dominates at 0.021 and 0.032 MHz (Fig. 9). Phase shift could offer good discrimination between RNA (control) and RNA (HCC). Nonlinear polarization could secure facile HCC diagnosis.

Ten signal measurements of the DNA (control), RNA (control), and RNA (HCC) responses were calculated into a histogram for the frequency distribution. The DNA (control), RNA (control), and RNA (HCC) all had standard deviations of 0.164, 0.155, and 0.146, respectively. The RNA (HCC), DNA (control), and RNA mean values

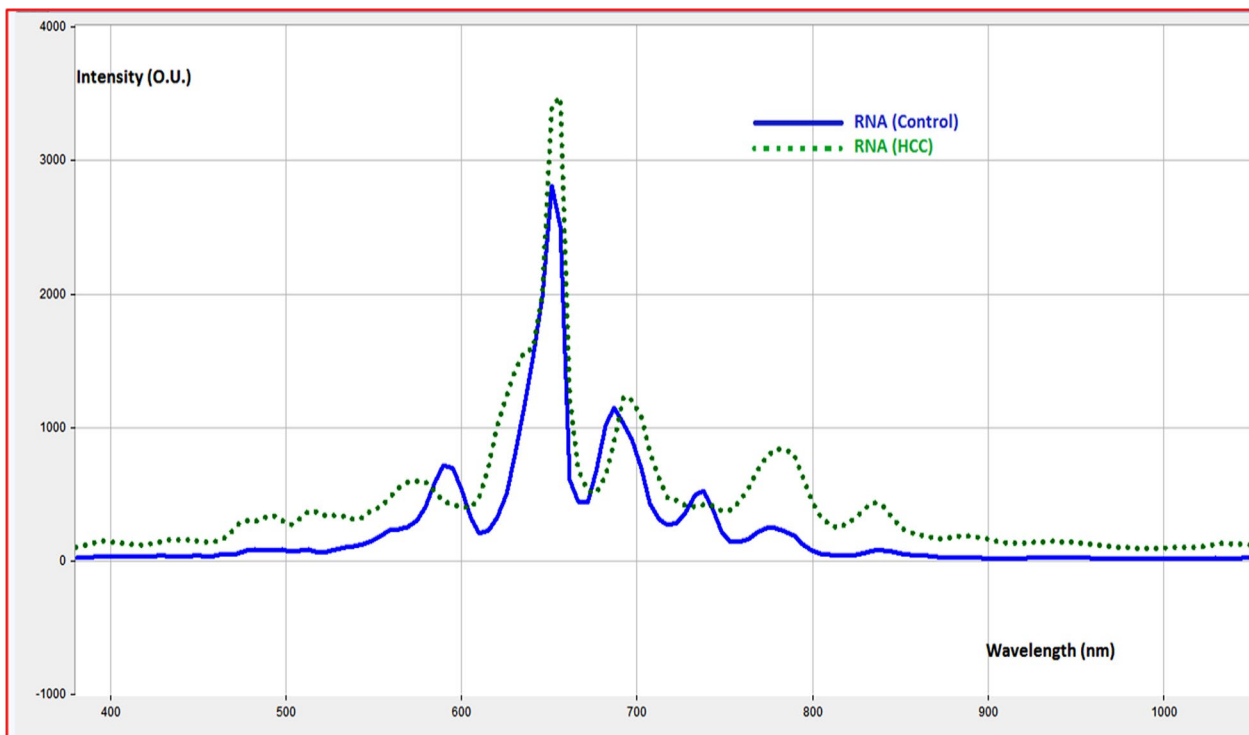


Fig. 6 Scattered and re-emitted radiation light of RNA (control) and RNA (HCC) after being irradiated with laser source at 656 nm

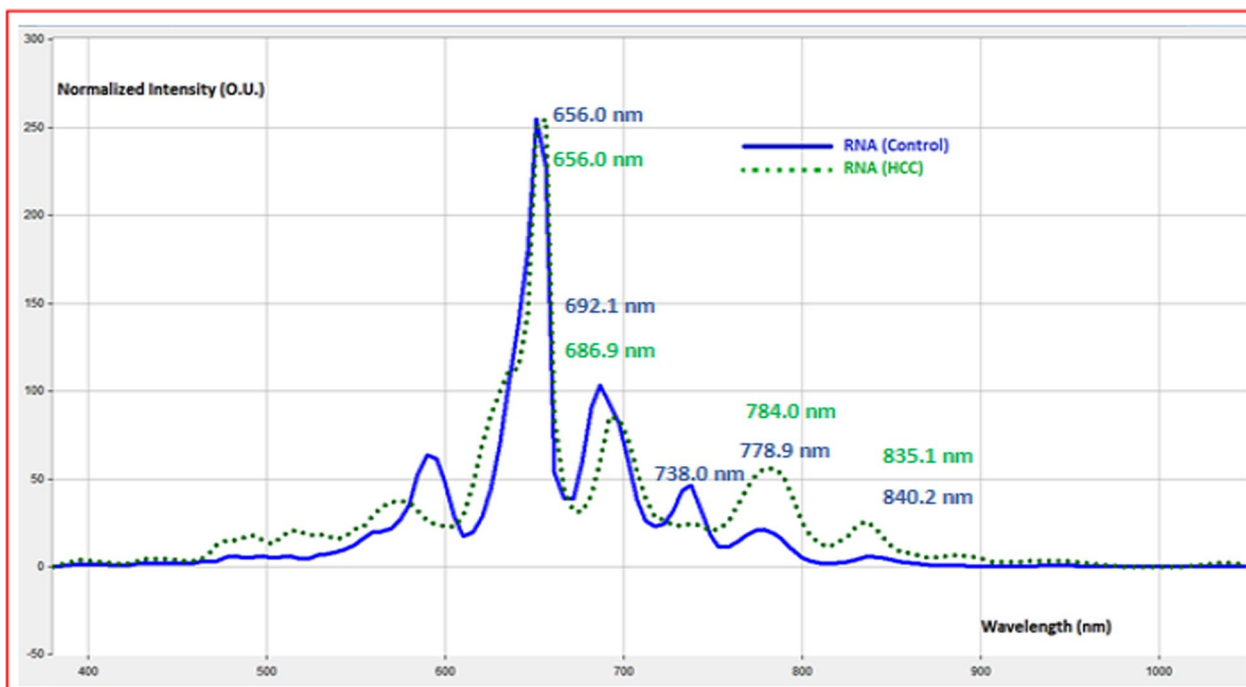


Fig. 7 Normalized scattered and re-emitted radiation light of RNA (control) and RNA (HCC) after being irradiated with laser source at 656 nm

Table 4 Characteristic light polarization signature of RNA (control) and RNA (HCC)

Sample	Rayleigh scattering (nm)	Re-emitted radiation (2nd harmonic) (nm)	Re-emitted radiation (3rd harmonic) (nm)	Re-emitted radiation (4th harmonic) (nm)	Re-emitted radiation (5th harmonic) (nm)
RNA (control)	656.0	692.1	738.0	778.9	840.2
RNA (HCC)	656.0	686.9	–	784.0	835.1

Table 5 Attenuation of transmitted light polarization (scattered and re-emitted) of RNA (Control) and RNA (HCC)

Sample	Rayleigh Scattering (Intensity a.u.)	Re-emitted radiation (2nd harmonic) (Intensity)	Re-emitted radiation (3rd harmonic) (Intensity)	Re-emitted radiation (4th harmonic) (Intensity)	Re-emitted radiation (5th harmonic) (intensity)
RNA (control)	3472.7	1208.4	417.9	841.0	85.0
RNA (HCC)	3807.2*	1150.1*	527.5*	252.1*	445.6*

are 0.091, 0.08, and 0.123, respectively. We notice that the mean values shift to right when the patient suffering from HCC cancer (Fig. 10).

Conclusion and future perspective

Nonlinear polarization secured characteristic signature of total DNA (control) and RNA (control). Total DNA demonstrated characteristic resonance frequency that differs from total RNA at 2nd, 3rd, 4th, 5th harmonic with different light attenuation. DNA demonstrated

characteristic spectrum frequency response lines starting from 0.0044 to 0.0118 GHz compared with RNA spectrum lines. While DNA demonstrated a phase shift dominates at 0.88 GHz, RNA leads at 0.106 GHz. These characteristic signatures could be employed to monitor any genetic changes related to HCC tumors. RNA (HCC) demonstrated phase shift at 0.014, 0.021, 0.032, and 0.072 MHz from RNA (control). This novel modality could pave the way for facile diagnosis of different tumors.

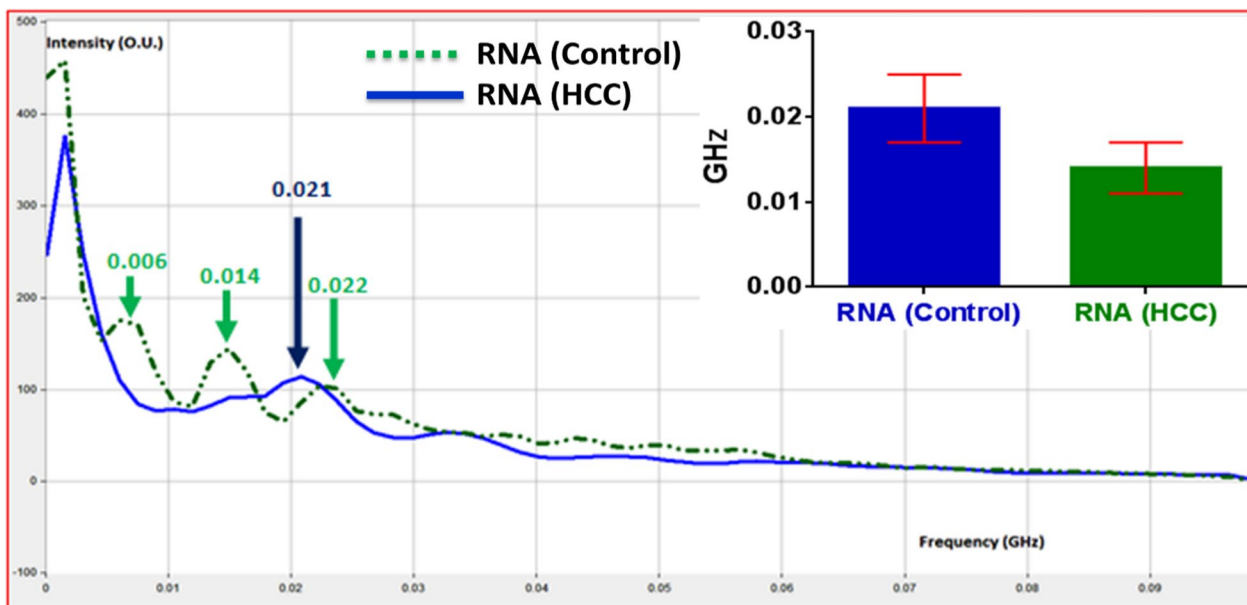


Fig. 8 Determination of RNA resonance frequency change due to HCC

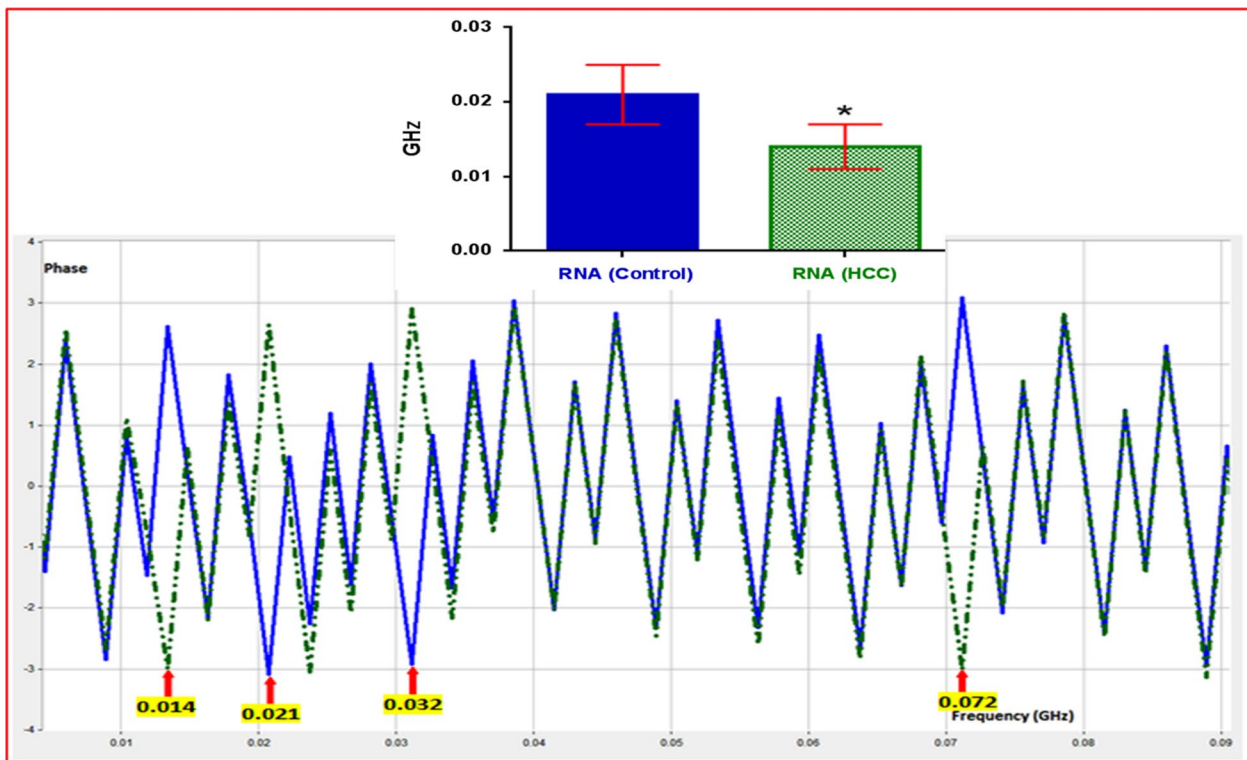


Fig. 9 Phase difference between RNA (control) and RNA (HCC)

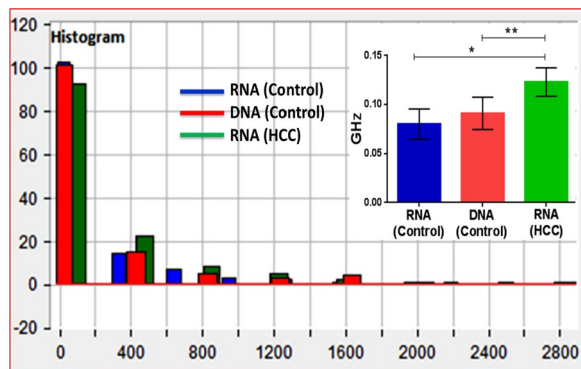


Fig. 10 The calculated histogram for RNA, DNA, and RNA (HCC)

Abbreviations

DNA	Deoxyribonucleic acid
EASL	European Association for the Study of the Liver
EDTA	Ethylenediaminetetraacetic acid
GHz	Gigahertz
HCC	Hepatocellular carcinoma
Hgb	Hemoglobin
HIS	Hyperspectral imaging
LED	Light-emitting diode
MHz	Megahertz
PLT	Platelet
RBC	Red blood cell
RNA	Ribonucleic acid
SD	Standard deviation
TLC	Total leukocyte count

Author contributions

Yasser H. El-Sharkawy suggested the research topic, investigated the article, planned the research methodology, wrote the original draft, and participated in data representation and article revising and editing. Sherif Elbasuney suggested the research topic, investigated the article, planned the research methodology, wrote the original draft, and participated in data representation and article revising and editing. Sara M. Radwan suggested the research topic, investigated the article, planned the research methodology, wrote the original draft, and participated in data representation and article revising and editing. Mostafa A. Askar suggested the research topic, investigated the article, planned the research methodology, wrote the original draft, and participated in data representation and article revising and editing. Samar H. Rizk suggested the research topic, investigated the article, planned the research methodology, wrote the original draft, and participated in data representation and article revising and editing. Gharieb S. El-Sayyad suggested the research topic, investigated the article, planned the research methodology, wrote the original draft, and participated in data representation and article revising and editing.

Funding

This research received no external funding.

Availability of data and materials

The data are available on request.

Declarations

Ethical approval and consent to participate

According to the Helsinki Declaration, all experimental and investigative trials were authorized by Cairo University's Ethical Committee of Research (P.T.REC/009/003144). Before data collection began, all participants read and signed two copies of a permission form.

Consent to publish

None.

Competing interests

According to the authors, there were no financial or commercial ties that would have created a conflict of interest when conducting the study.

Received: 6 July 2023 Accepted: 14 June 2024

Published online: 22 June 2024

References

- Zhang Y, Wen G-M, Wu C-A, Jing Z-L, Li D-Z, Liu G-L, Wei X-X, Tang M-S, Li Y-H, Zhong Y, Deng Y-J, Yang W-K (2019) PRKDC is a prognostic marker for poor survival in gastric cancer patients and regulates DNA damage response. *Pathol Res Pract* 215(8):152509
- Hu G, Li P, Cui X, Li Y, Zhang J, Zhai X, Yu S, Tang S, Zhao Z, Wang J, Jia G (2018) Cr(VI)-induced methylation and down-regulation of DNA repair genes and its association with markers of genetic damage in workers and 16HBE cells. *Environ Pollut* 238:833–843
- Jianfeng W, Yutao W, Jianbin B (2021) Long non-coding RNAs correlate with genomic stability in prostate cancer: a clinical outcome and survival analysis. *Genomics* 113:3141–3151
- Hulstaert E, Morlion A, Levanon K, Vandessompele J, Mestdagh P (2021) Candidate RNA biomarkers in biofluids for early diagnosis of ovarian cancer: a systematic review. *Gynecol Oncol* 160(2):633–642
- Yang M, Wei S, Zhao H, Zhou D, Cui X (2021) The role of miRNA125b in the progression of hepatocellular carcinoma. *Clin Res Hepatol Gastroenterol* 45:101712
- Gao T-M, Bai D-S, Qian J-J, Zhang C, Jin S-J, Jiang G-Q (2021) The growth rate of hepatocellular carcinoma is different with different TNM stages at diagnosis. *Hepatob Pancreat Dis Int* 20:330–336
- Cunha GM, Fowler KJ, Abushamat F, Sirlin CB, Kono Y (2020) Imaging diagnosis of hepatocellular carcinoma: the liver imaging reporting and data system, why and how? *Clin Liver Dis* 24(4):623–636
- York T, Powell SB, Gao S, Kahan L, Charanya T, Saha D, Roberts NW, Cronin TW, Marshall J, Achilefu S, Lake SP, Raman B, Gruev V (2014) Bioinspired polarization imaging sensors: from circuits and optics to signal processing algorithms and biomedical applications: analysis at the focal plane emulates nature's method in sensors to image and diagnose with polarized light. *Proc IEEE Inst Electr Electron Eng* 102(10):1450–1469
- Wang Y, Louie DC, Cai J, Tchvialeva L, Lui H, Jane Wang Z, Lee TK (2021) Deep learning enhances polarization speckle for in vivo skin cancer detection. *Opt Laser Technol* 140:107006
- Offerhaus HL, Bohndiek SE, Harvey AR (2018) Hyperspectral imaging in biomedical applications. *J Opt* 21(1):010202
- Kur E, Lazarow M, Wurtele JS, Michel A (2021) Nonlinear polarization transfer and control of two laser beams overlapping in a uniform nonlinear medium. *Opt Express* 29:1162–1174
- Gopal AA, Kazarine A, Dubach JM, Wiseman PW (2021) Recent advances in nonlinear microscopy: deep insights and polarized revelations. *Int J Biochem Cell Biol* 130:105896
- Wyatt PJ (2021) Differential light scattering and the measurement of molecules and nanoparticles: a review. *Anal Chim Acta: X* 7:100070
- Yahia IS, Zahran HY, Alamri FH (2017) Linear and nonlinear optics of pyronin Y/flexible polymer substrate for flexible organic technology: new optical approach. *Opt Laser Technol* 95:124–132
- Han J, Liu X, Jiang M, Wang Z, Xu M (2021) An improved on-line measurement method of particulate matter concentration using tri-wavelength laser light scattering. *Fuel* 302:121197
- Schärtl W (2007) Light scattering from polymer solutions and nanoparticle dispersions. Springer, Berlin
- Lokstein H, Leupold D, Voigt B, Nowak F, Ehlert J, Hoffmann P, Garab G (1995) Nonlinear polarization spectroscopy in the frequency domain of light-harvesting complex II: absorption band substructure and exciton dynamics. *Biophys J* 69(4):1536–1543
- Badiyan S, Ameri A, Razzaghi MR, Rafii-Tabar H, Sasanpour P (2019) Mueller matrix imaging of prostate bulk tissues. Polarization parameters as a discriminating benchmark, Photodiagnosis and Photodynamic Therapy 26:90–96
- Krikunova M, Voigt B, Lokstein H (2002) Direct evidence for excitonically coupled chlorophylls a and b in LHC II of higher plants by nonlinear

- polarization spectroscopy in the frequency domain. *Biochim Biophys Acta (BBA) Bioenerg* 1556(1):1–5
20. El-Sharkawy Y (2015) Design and implementation of noninvasive laser imaging system for human teeth carious detection and removal. *J Dent Lasers* 9(2):80–88
 21. El-Sharkawy YH, El-Sherif AF (2014) High-performance near-infrared imaging for breast cancer detection. *J Biomed Opt* 19:016018
 22. El-Sharkawy YH, Elbasuney S (2020) Tunable laser-induced fluorescence with signal correlation algorithm for dental caries detection with controlled ablation. *Opt Laser Technol* 129:106299
 23. Lu G, Fei B (2014) Medical hyperspectral imaging: a review. *J Biomed Opt* 19(1):010901
 24. Rehman AU, Qureshi SA (2021) A review of the medical hyperspectral imaging systems and unmixing algorithms' in biological tissues. *Photodiagn Photodyn Ther* 33:102165
 25. Aboughaleb IH, Aref MH, El-Sharkawy YH (2020) Hyperspectral imaging for diagnosis and detection of ex-vivo breast cancer. *Photodiagn Photodyn Ther* 31:101922
 26. Zheludev V, Pölonen I, Neittaanmäki-Perttu N, Averbuch A, Neittaanmäki P, Grönroos M, Saari H (2015) Delineation of malignant skin tumors by hyperspectral imaging using diffusion maps dimensionality reduction. *Biomed Signal Process Control* 16:48–60
 27. Hashimoto E, Ishikawa M, Shinoda K, Hasegawa M, Komagata H, Kobayashi N, Mochidome N, Oda Y, Iwamoto C, Ohuchida K (2017) Tissue classification of liver pathological tissue specimens image using spectral features. In: *Medical imaging 2017: digital pathology*, SPIE, 2017, pp 243–248
 28. Du L, Dai Y, Sun Z (2020) Twisting for tunable nonlinear optics. *Matter* 3(4):987–988

Publisher's Note

Springer Nature remains neutral with regard to jurisdictional claims in published maps and institutional affiliations.